Int. J. Nanoelectronics and Materials **2** (2009) 173-182

Electronic and optical properties of the express purified SWCNTs produced by HiPCO process

Badis Bendjemil*

LEREC, University of Badji-Mokhtar, B. P. 12, 23000 Annaba, Algeria
University of 8 May 1945 Guelma, B. P. 401, 24000 Guelma, Algeria
IFW-Dresden, Helmholtzstraß 20 D-01069 Dresden, Germany

Abstract

Single-walled carbon nanotubes have been synthesized by a gas-phase CO decomposition (HiPCO) process, involving high-pressure disproportionation of CO as carbon feedstock and catalytic iron particles were obtained from pyrolysis of $Fe(CO)_5$. The diameter and diameter distribution of as grown material dependents on various parameters, the strong is the pressure of CO cold transverse the $Fe(CO)_5$, nozzle geometry and position for the injection of the reactant in the reaction chamber to produce smaller diameter (about 0.9 nm) at higher CO pressure. The HiPCO materials containing iron were purified by a two-step process of oxidation in oxygen atmosphere and successive washing the mixture of hydrochloric and nitric acids neutralised and distilled water (1:1:1). The optical and electronic properties were studied using optical absorption and infrared spectroscopy; in addition, high-resolution transmission electron energy-loss spectroscopy was used to analyse the loss function, electron diffraction and core level excitations. The degree of purification achieved was estimated using transmission electron microscopy. Furthermore, the present procedure has a no sufficiently change in the diameter and diameter distribution after Gaussian fit of the optical absorbance spectra. The estimation of the degree of purification is possible by the analysis of core level excitation; finally high purity SWCNTs were obtained.

Keywords: Gaussian fit**;** Loss function; High Resolution Electron energy loss spectroscopy.
PACS: 81.20.Ka; 74.70.-b; 75.50.-y.

1. Introduction

Single-wall carbon nanotubes (SWCNTs) [1], have attracted interest as a new one-dimensional material, due to their exceptional electronic [2] and mechanical properties [4] which make them promising candidates for applications in nano-scale technologies. Many methods of production have been studied. SWCNTs have been produced by laser ablation [5-7] and arc discharge [8-9], catalytic decomposition of hydrocarbons [10-11] and microwave plasma assisted by CVD with [12] and without hot filament [13]; in addition SWCNTs and MWCNTs by SHS and electro-thermal explosion reactions [14]. The SWCNTs with purity about 90 wt % have been formed from the gas phase using the Ferrocene $Fe(CO)_5$ with high pressure of CO through the high-pressure disproportionation of CO process (HiPCO) [15, 18].

*) For Correspondence, E-mail: badis23@yahoo.fr

In this process, Fe $(CO)_5$ is injected into a stream of CO gas at high temperatures between 900 and 1150°C and pressures between 1 and 40 bar The iron forms metal clusters that act as catalytic sites to promote the Boudouard reaction.

$$\mathbf{COc + COh \rightarrow C\ (solid) + CO_2\ (gas)} \quad (1)$$

And when the metal clusters achieve a size near that of C_{60}, they nucleate and grown SWCNTS. The SWCNTS will continue to grow until the metal cluster, which is also growing with addition of residual free iron atoms. The average diameter of SWCNTs grown using the HiPCO method is a function of CO pressure, but is usually < 1 nm, which is pure and smaller than SWCNTs synthesized by the laser vaporisation process. The as-grown synthesized carbon nanotubes contain a considerable amount of impurities such as iron cluster catalyst particles, amorphous and other forms of carbon [23-29] These impurities represent a serious impediment to a detailed surface characterization and the transformation of the nanotubes in regard to their potential applications. Several purification procedures [16-23] including acid treatments and annealing in air [25-29] , oxidation in an oxygen atmosphere and wet with argon and washing with different solvent and acid [25, 26, 30-32], high temperature annealing [33-34] and finally oxidation of the iron clusters with flash ignition [34]. All these purification procedures were been aimed at removing particular impurities and without loss weighs, previous study of the evolution of the surface area and absorption isotherm of the gas [36-37] and evolution of the pore structure [38] are also related. Much effort has been applied to use for increase the yield and purity can be improved by addition of gases such as hydrogen and acetylene [39]. In this work we report a purification procedure with a high yield (about 90%) and minimum weight loss using oxidation in an oxygen atmosphere followed by washing in the neutralised HCl (36 % MU), HNO_3 (60 %) distilled water (1:1:1) sonicated at 80 C° above experimental 15 mn and then neutralised. The bundles of the SWCNTs contain metallic iron impurities with 5 to 10 nm size of nanoparticles is encased in carbon shells and with 10 wt % and other form of carbon. We have demonstrated that this leads to SWCNTs materials without carbonacious impurities and express complete removal of the catalyst iron and iron oxide present in the sample The aim of our purification is to oxidise the iron, amorphous carbon and carbonaceous species by selective oxidation in an oxygen atmosphere and successive washing with the purification solution sonicated above experimental 15 mn at T= 80 C°. In order to dissolve iron catalyst metallic and oxide form from the as grown carbon nanotubes with minimal loss of SWCNTs is obtain.

2. Experimental

The as grown material with the optimal synthesis parameters containing 90 wt % SWCNTs with optimal parameters (average diameter, diameter distribution), (temperature, CO pressure and nozzle diameter, geometry and position) reported in the reference [18]. The as produced SWCNTs contain catalyst particles (about 10 %), amorphous and other forms of carbon. In order to purify the sample, two different steps [43, 44] have been applied. Firstly, oxygen (99,999 % purity) was fed into the quartz tube via a leak valve up to a partial oxygen pressure of $5x10^{-6}$ mbar at a temperature between 200 C° and 800 C°, while the annealing time was 12 to 48 h. Within these ranges we have systematically varied the

parameters in order to optimise the degree and yield of the purification process. The optimal parameter set was found to be a 12 h annealing at 500 C° without loss of SWCNTs.

Finally, the nanotubes were taken out of the quartz tube and immersed or refluxed in the purification solution. The solution was then neutralized and filtered through the Buck paper and drained in vacuum. In order to obtain thin films for the microscopy and spectroscopic studies, the nanotubes were dispersed ultrasonically in ethanol and dropped onto NaCl single crystals. The films were then characterized as regards to their optical response using a BRUKER IFS 88 spectrometer. The resolution was set to 2 cm^{-1} (0.25 meV). For transmission electron microscopy (HRTEM) including electron high-energy loss spectroscopy (HREELS) to analyse loss function, electron diffraction and the core level excitation, the films were floated off in distilled water and mounted on standard platinum grids. The HRTEM and HREELS studies were performed respectively in a Philips CM20FEG electron microscope and in purpose-built high-energy electron energy -loss spectrometer in transmission described elsewhere [44].

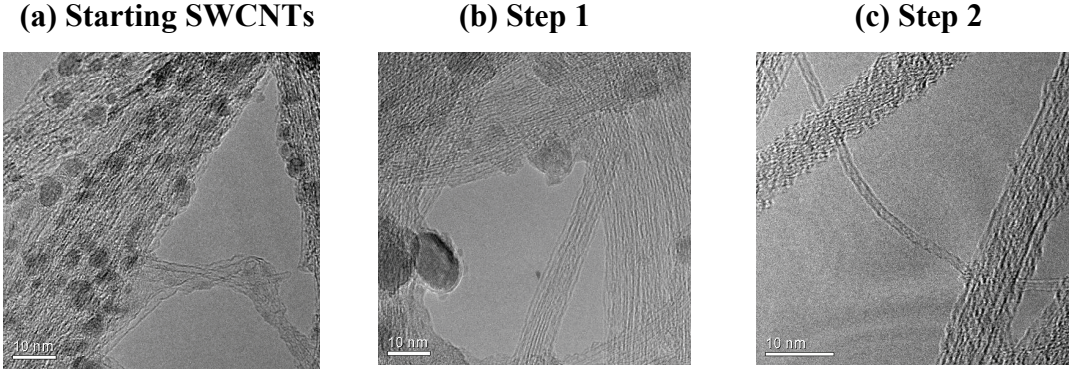

Fig. 1: High resolution TEM imaging of, a- the as grown SWCNTs, b- after oxidation in oxygen atmosphere at T= 500 °C, P = 5.10^{-6} mbar during 12h (step1), c- after chemical purification using HCL and HNO_3 mixed with water (step2).

3. Results and Discussion

Fig.1a shows typical HRTEM pictures of the as grown HiPCO materials, revealing a fine and homogeneous distribution of the iron catalyst nanoparticles. This is in agreement with the HiPCO-SWCNTs behaviour in oxidation treatments that it is more stable at higher temperature, open and exposes the iron to oxidize. The iron oxide is characterized by lower density and acid solution has ability to extract it, comparatively to the bigger iron density, reported by [25]. The optimal parameter of our oxidation treatments is at T= 500 °C under low pressure of 5.10^{-5} mbar for 12 h (step 1) and after washing in the solution of the purification (step 2). From Fig.1 the purification process applied successfully removes most of impurities is still seen in Fig.1a as spherical, fine and homogeneous catalyst iron nanoparticle (with diameter of 5 nm) are oxidized in the second step of our treatment. The oxides are evident in the TEM image (with diameter of 10 nm). After washing in the purification solution we can observe no sign of any catalyst nanoparticle, and we see only trace of amorphous carbon.

In Fig.2 we shows the optical absorbance spectra characteristic of the nanotubes before and after oxidation treatments steps at the optimal temperature 500 °C during the oxidation time from 12 to 36 hours. The increasing of the absorbance of SWCNTs is result of the oxidation of the amorphous carbon observed in the area of the first optical interband semiconductor transition peak (E_{11}^{S}) and the presence of the iron clusters oxides in the sample decreased the intensity of the second optical interband semiconductor transition peak (E_{22}^{S}) with more oxidation time the spectra shift to lower energy. This is the consequence of increasing of the SWCNTs diameter by oxidation of small diameter. These contribute to the decreasing of the absorbance spectra which has been confirmed in previous studies [43, 44]. The optimal parameter in this was found at 12 h, remaining of diameter and diameter distribution and increasing of the relative SWCNTs absorbance respectively in comparison with the as grown HiPCO materials. After immersion of the optimally oxidized SWCNTs in the purification solution, we observe the evolution of the relative absorbance of the SWCNTs in the sample. This can be explaining by the removal of iron and iron oxide from our samples during the purification. The relative nanotubes concentration in the samples increase and the diameter remain constant because the SWCNTs are more stable in this temperature and time. Optical absorbance spectroscopy is a bulk scale technique, which can give information about diameter and diameter distributions of the SWCNTs. The yield of SWCNTs is characterized by the area of the absorbance spectra peak, after the Gaussian fit of the fine structure of semiconductor peak E_{22}^{S} [45]

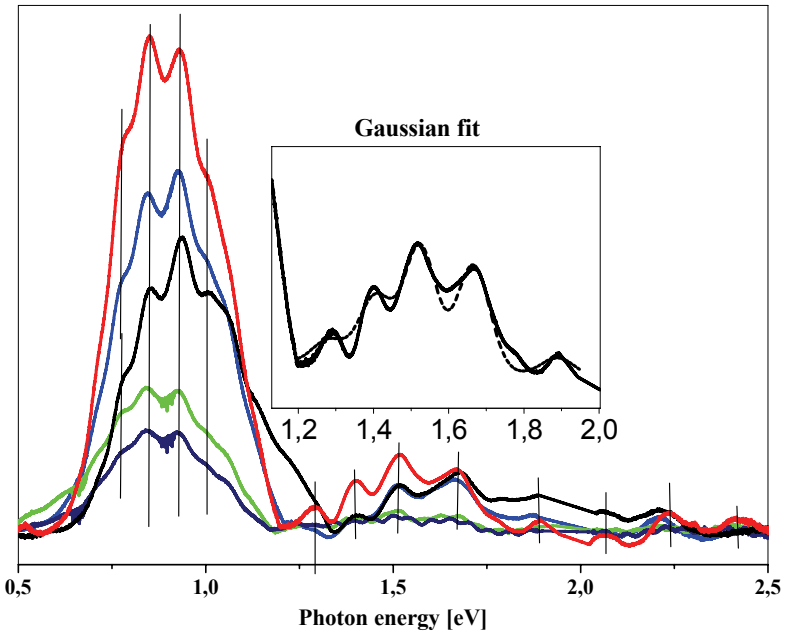

Fig. 2: The optical absorbance spectra of as-grown SWCNTs (black), after 12h oxidation (blue), after 24 h oxidation (green) and after 36 h oxidation (navy) and after chemical purification (red). Gaussian fit of the E_{22}^{S} peak dashed line, which is presented in the inset.

As grown HiPCO materials are characterized by a larger distribution of the diameter compared to SWCNTS made by laser vaporisation technique. This can be explained by the fluctuation of the synthesis temperature and by the position of nozzle in the reaction chamber. The structures seen in the optical absorbance spectra are related to interband excitations between the π derived van Hove singularities in the density of states (DOS) of the nanotubes [49].

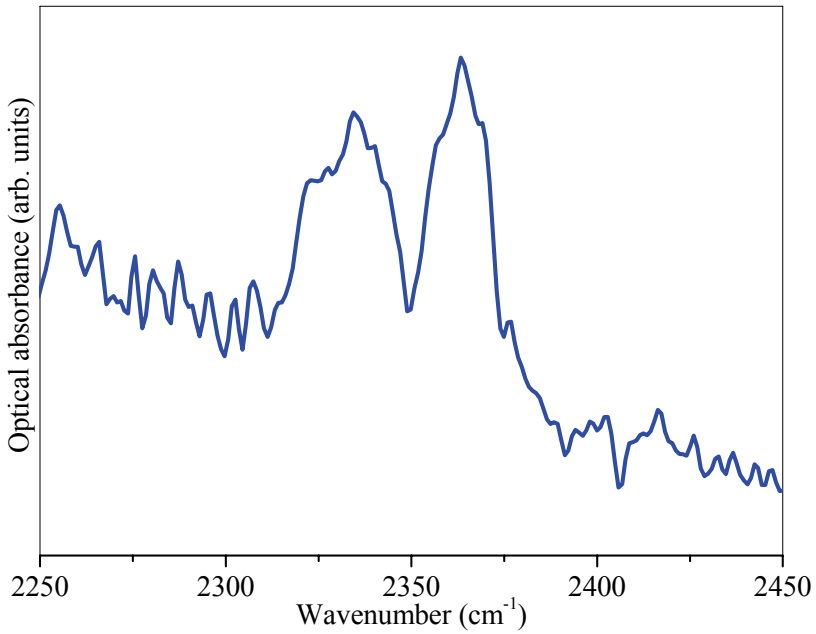

Fig. 3: Infrared response of HiPCO SWCNTs after oxidation treatment (blue).

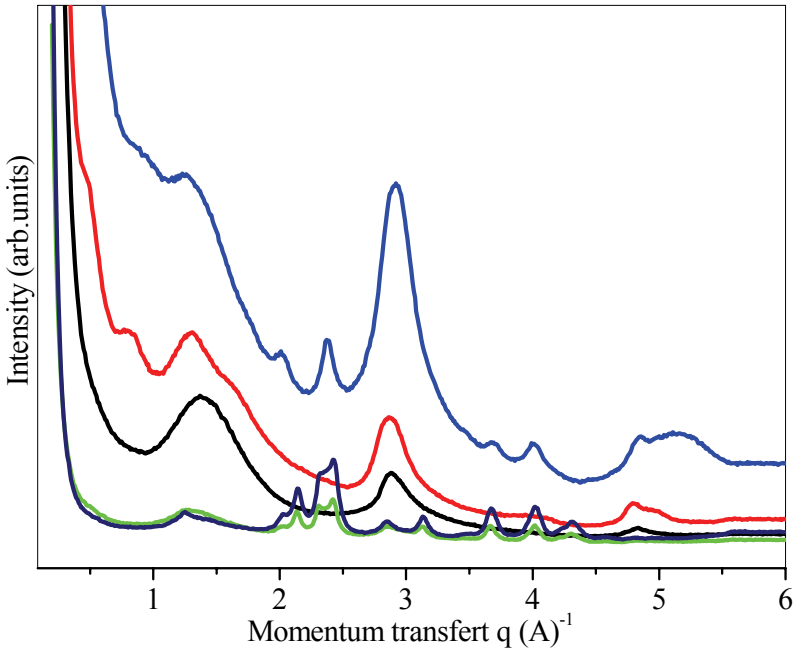

Fig. 4: Electron diffraction spectra of the as grown SWCNT, of as-grown SWCNTs (black), after 12h oxidation (blue), after 24 h oxidation (green), after 36 h oxidation (navy) and purified (red).

Fig.3 shows typical infrared absorbance spectra response of the iron oxide hematite (Fe_2O_3) after oxidation treatments, located at the vibration phonons 2321, 2334 and 2363 cm^{-1} according to the reference [3], correspond to the longitudinal and transverse optical phonon modes. In Fig.5 we show the electron diffraction pattern of the as-grown nanotubes, the SWCNTs after the oxidation steps and after immersion in the purification solution. The as-grown SWCNTs are characterized by small electron diffraction intensity of the triangular lattice small rope; the features are located at 2.87 and 4.92 A^{-1} corresponding to (100) and (110) graphite in-plane reflections [48, 49]. After oxidation, the diffraction is dominated by the appearance of new features at 1.25, 2.13, 2.41, 3.12, 3.67, 3.98, 4.01, 4.32, 4.59, 4.85, 5.16 A^{-1} corresponding to Fe_2O_3 (confirmed by infrared spectroscopy response and represented in the HRTEM pictures). With more oxidation time the oxide became dense. After immersion in the purification solvent this oxide is completely removed and the peaks intensity of ropes is increased, diffraction located at about 0.45, 0.83 and 1.24 A^{-1}, corresponding to the reflection planes (100), (110) and (210) which are reflecting the structure of the individual tubes with small bundles [49]. These results assigned the degrees of the proposed purification procedure (Fig.4).

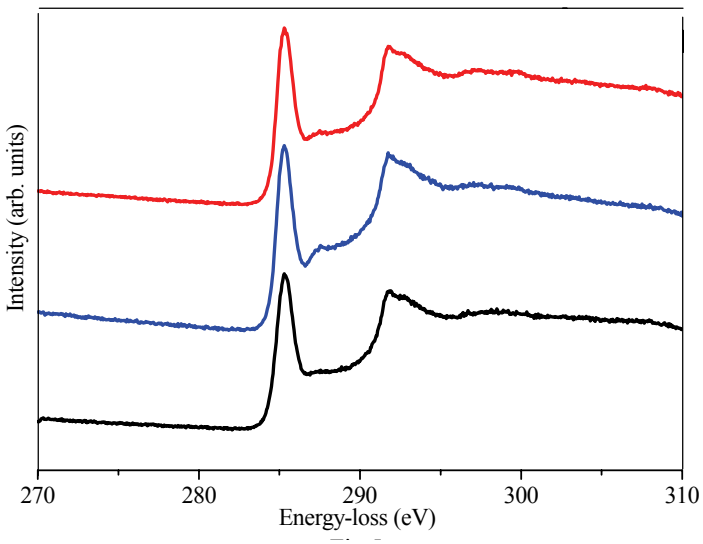

Fig. 5a: High energy-resolution EELS core level excitation of C_{1s}, as grown SWCNTs (black), after 12h oxidation (blue) and after purification (red).

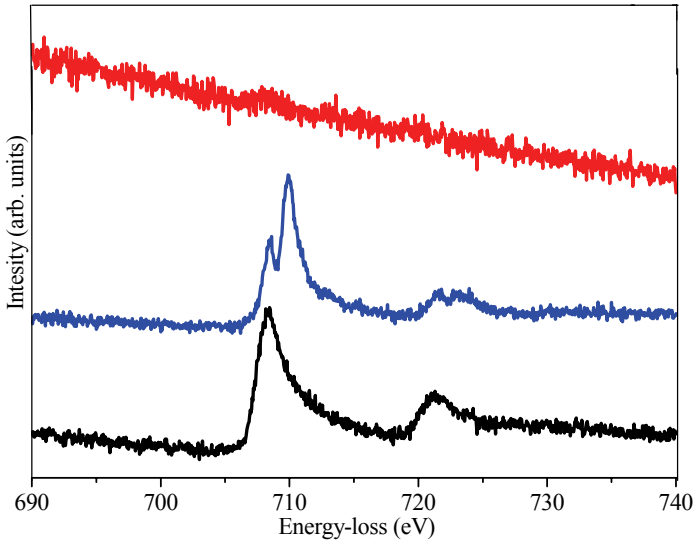

Fig. 5b: High energy-resolution EELS core level excitation of O_k, as grown SWCNTs (black), after 12h oxidation (blue) and after purification (red).

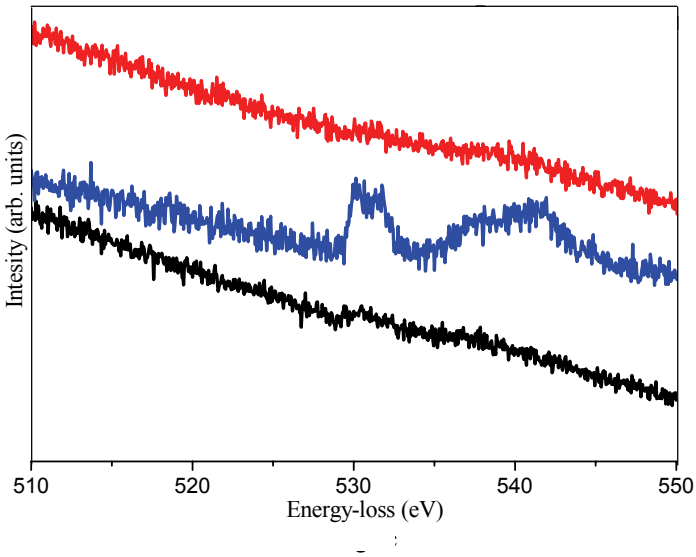

Fig. 5c: High energy-resolution EELS core level excitation of Fe_{2p}, as grown SWCNTs (black), after 12h oxidation (blue) and after purification (red).

EELS spectra confirm the presence of carbon, iron and their oxide (Fig.5):-C_{1s} (carbon seuil) of SWCNTs (sp_2 hybridation) characterized by the excitations, $1s\rightarrow\pi^*$ and $1s\rightarrow\sigma^*$ (excitations from s seuil to orbitals molecular π and σ) at 285.2 and 293 eV respectively (Fig.5a) see reference [50] of (as grown SWCNTs, oxidized and purified). The electron density of the unoccupied stat π^* after purification demonstrate the purity of SWCNTs, without defect and high electronic excitation assigned by the occupied stat π bond.

-Fe_{2P} shows the excitation of the iron in metallic and oxide forms corresponding to the as grown, oxidized and purified SWCNTs (Fig.5a). Only metallic $Fe_{2p1/2}$ and $Fe_{2p3/2}$ asymmetric peaks characterize the as-grown materials, because the iron is not bonded with

oxygen and it is related to the density of states at the loss energy of 708 and 721 eV, respectively [51, 52]. On the other hand, the oxidized sample shows the typical Fe_{2P} peak of hematite Fe_2O_3, confirmed by IR spectra (Fig.3) in which the peak became symmetric, with same remaining metallic iron in the sample after oxidation.

In the range of energy 711 and 724 eV [51, 52]. This is also confirmed by X ray photoelectron spectroscopy in the previous studies [40, 53].
-O_k shows the excitation of the oxygen peaks located at 530 and 540 eV, this have been observed in loss function spectra after washing in the purification solution has no signature of oxygen and iron metallic or oxide peaks (Fig.5c)..

3. Summary

In summary, we have express purified SWCNTs using purification procedure manufactured a two-step, consisting of oxidation in oxygen atmosphere and subsequent immersion in mixed and neutralised acid HNO_3 and HCl with distilled water. We proved that after an optimisation of the oxidation treatments parameters the purification successfully removes amorphous carbon as well as iron catalyst nanoparticles. The high overall yield of the purification renders the procedure applicable for large-scale purification.

Acknowledgements

I am grateful to the DAAD (German Academic Exchange Service) for financial support. I would like to express my special thanks to Prof. Jörg Fink and Drs. Martin Knupfer, Heiko Peisert, Thomas Pichler, Albrecht Leonhardt and Dietmar Selbmann for making my thesis possible at the Institute and for supporting it with interest. Many thanks go to the technical staff, Gesine Kreutzer, Sieglinde Pichl, Stephan Leger, Kerstin Müller and Roland Hübel. The spectroscopy group members, Drs. Sergey Borisenko, Ewa Borowiac-Palen, Xianjie Liu, Garcia Fuentes, Andrik Rauf and Mark Herman Rummeli.

Professor Odile Stéphan from the ULTRA-STEM Group-Laboratory of solid state Physics (UMR 8502), university Paris-Sud-Orsay, are also acknowledged for the ultra-STEM pictures and analysis. We hope for soon with Professor Odile Stéphan a future collaboration in activation of the purified SWCNTs by (intercallation, doping and filling) for biomedical and nanotechnology´s applications.

References

[1] S. Iijima, T. Ichihashi, Nature **363** (1993) 603
[2] R. Saito, G. Dresselhaus, M. S. Dresselhaus, Physical properties of carbon nanotubes (Imperial College, London 1998)
[3] A. N. Richard, L. P. Curtis, M. A. Leugers, The handbook of infrared and Raman spectra of inorganic compounds and organic salts (volume **2**, London 1988)
[4] J. P. Salvetat, J. M. Bonard, N. H. Thomson, A. J. Kulik, L. Forró, W. Benoit, L. Zuppiroli, Appl. Phys. A **69** (1999) 225
[5] A. Thess, R. Lee, P. Nikolaev, H. Dai, P. Petit, J. Robert, C. Xu, H. Lee, S. G. Kim, D. T. Colbert, G. Scuseria, D. Tomarek, J. E. Fischer, R. E. Smalley, Science (1996) 483
[6] Rinzler, A. G., J. Liu, H. Dai, P. Nikolaev, C. B. Huffman, F. J. Rodriguez-Macias, P. J. Boul, A. H. Lu, D. Heymann, D. T. Colbert, R. S. Lee, J. E. Fischer, A. M. Rao,

P. C. Eklund & R. E. Smalley, Applied Physics a-Materials Science & Processing **67**, (1998) 29
[7] T. Guo, P. Nikolaev, A. Thess, D. T. Colbert, R. E. Smalley, Chem. Phys. Lett. **243** (1995) 49
[8] C. Journet, W. K. masser, P. Bernier, A. Loiseau, M. Lamy de la chapelle, S. Lefrant, P. Deniard, R. S. Lee, J .E. Fischer, Nature **388** (1997) 756
[9] S. Iijima: Nature **354** (1991) 56
[10] J. H Hafner, M. J. Bronikowski, B. R. Azamian, P. Nikolaev, A. G.Rinzler, D.T. Colbert, K. A. Smith, R. E. Smalley, Chem. Phys. Lett. **296** (1998) 195
[11] J. F. Colomer, G. Bister, I. Willems, Z. Konya, Fonsera, G. VanTendeloo, J. B. Nagy: Chem. Comm, (1999) 1343
[12] S. Rizk, M. B. Assouar, M. Belmahi, L. Le Brizoual, J. Bougdira, physica status solidi, **204**, (2007) 3085
[13] P. Špatenka, F. Pàcal, Ch. Täschner, A. Leonhardt, J. Blazek, J. Phys. D: Appl. Phys. **37** (2004) 2709
[14] N. I. Alekseev, S. G. Izotova, Yu. G. Osipov, S. V. Polovtsev, K. N. Semenov, A. K. Sirotkin, N. A. Charykov, S. A. Kernozhitskaya, Technical physics, **2** (2006) 231
[15] P. Nikolaev, M. J. Bronikowski, R.. K. Bradley, F. Rohmound, D. T. Colbert, A. K. Smith, R. E. Smalley, Chem. Phys. Lett. **313** (1999) 91
[16] H. M. Cheng, F. Li, X. Sun, SDM. Brown, M. A. Pimenta, A. Marucci, G. Dresselhaus, M. S. Dreselhaus, Chem. Phys. Lett **289** (1998) 602
[17] M. J. Bronikowski, P. A. Willis, D. T. Colbert, K. A. Smith, R. E. Smalley, J. Vac. Sci. Technol. A **19** (4), (2001) 1800
[18] D. Selbmann, B. Bendjemil, A. Leonhardt, T. Pichler, Ch. Täschner, M. Ritschel, Applied Physics A, Materials Science and Processing **90** (2008) 637
[19] H. Hidefumi, Mol. Cryst. Liq. Cryst. Sci. Technol., Sect. **A 276** (1995) 267
[20] M. Yumura, K. Uchida, H. Niino, S. Ohshima, Y. kuriki, K. Yase, F. Ikazaki: Mater. Res. Soc. Symp. Proc. Novel Forms of carbon II **349** (1994) 231
[21] A. Dillon, T. Gennett, K. Jones, J. Alleman, P. Parilla, M. Heban, Adv. Mater.**16** (1999) 1354
[22] S. Bandow, Z. Zhao, Y. Ando: Appl. Phys. A **67** (1999) 23
[23] A. Rinzler, J. Liu, H. Dai, P. Nikolaev, C. Huffman, F. Rodriguez-Matias, P. Boul, A. Lu, D. Heymann, D. Colbert, Materials Science & Processing, Applied Physics **A 67**, (1998) 29
[24] R. Lee, J. Fischer, A. Rao, P. Eklund, R. E. Smalley, Appl. Phys A **67** (1998) 29
[25] E. Dujardin, T. Ebbesen, A. Krishnan, M. Treacy, Adv. Mater.**10** (1998) 611
[26] H. Hiura, T. Ebbesen, T. Tanigaki, Adv. Mater.**7** (1995) 275
[27] J. Zimmerman, R. Bradley, C. Huffman, R. H. Hauge, J. L. Margrave, Chem. Mater.**12** (2000) 1361
[28] W Chiang, B. E Brinson, A. Y. Huang, P. A Willis, M. J Bronikowski, J. L. Margrave, R. E Smalley, R. H. Hauge. J. Phys. Chem B **105** (2001) 8297
[29] M. T. Martìnez, M. A. Callejas, A. M. Benito, M. Cochet, T. Seeger, A. Anson, J. Schreiber, C. Gordon, C. Marhic, O.Chauvet, J.L.G. Fierro, W. K. Maser, Carbon **41** (2003) 2247
[30] C. M Yang, K. Kaneko, M. Yudazaka, S. Iijima, Nanoletters **2** (2002) 385
[31] V. A. Karachevtsev, A. Yu. Glamazda, U. Dettlaff-Weglikowska, V. S. Kurnosov, E. D. Obraztsova, A. V. Peschanskii, V. V. Eremenko, S. Roth. Carbon **41** (2003) 1567

[32] W. Zhou, Y. H. Ooi, R. Russo, P. Papanek, D. E. Luzzi, J. E. Fischer, M. J. Bronikowski, P. A. Willis, R. E, Smalley: Chem. Phys. Lett. **350** (2001) 6
[33] P. C .J. Graat, M. A. J, Somers. Appl.surf. Sci **100** (1996) 36
[34] S. J Roosendaal, B. V: Asselen , J. W. Elsenaar, A. M: Vredenberg, F. H. P. M: Habraken, Surf. Sci. **442** (1999) 329
[35] L. G. Bulusheva, A. V. Okotrub, U. Dettlaff-Weglikowska, S. Roth, M. I. Heggie, Carbon, carbon **42**, (2004) 1095
[36] M. Yudasaka, T. Ichihashi, D. Kasuya, H. Kataura, S. Iijima, Carbon **41** (2003) 1273
[37] M. Yudasaka, H. Kataura, T. Ichihashi, L. C. Qin, S. Kar, S. Iijima, Nanoletters **1** (2001) 487
[38] J. Smits, B. Wincheski, M. Namkung, R. Crooks, R. Louie, Materials Science and Engineering A **358** (2003) 384
[39] M. Cinke, J. Li, B. Chen, A. Cassell, L. Delzeit, J. Han , M. Meyyappan, Chem. Phy. Lett **365** (2002) 69
[40] C. M Yang, K. Kaneko, M. Yudasaka, S. Iijima: Physica B, Condensed Matter, **323** (2002) 140
[41] S. Shiraishi, H. Kurihara, K. Okabe, D. Hulicova, A. Oya, Electrochemistry Communications, (2002) 593
[42] K. Bladh, L. K. L. Falk, F. Rohmund, Appl. phys. A **70** (2000) 317
[43] B. Bendjemil, E. Borowiak-Palen, A. Graff, T. Pichler, M. Guerioune, J. Fink, M. Knupfer, Appl. Phy. A **78** (2004) 311
[44] E. Borowiak-Palen, T. Pichler, X. Liu, M. Knupfer, A. Graff, O. Jost, W. Pompe, R. J. Kalenczuk, J. Fink, Chem. Phys. Lett. **363** (2002) 567
[45] H. Kataura, Y. Kumazawa, Y. Maniwa, I. Umezu, Y. Ohtsuka, Y. Achiba, Synth. Met. **103** (1999) 2555
[46] M. Xia, S. Zhang, S. Zhao, E. Zhang, Physica B, B **344** (2004) 66
[47] J. Fink, Recent Development in Energy-Loss Spectroscopy. Ad. Electronics and Electron Physics, Vol. **75**, 121 (1989)
[48] B. W. Smith, Z. Benes, D. E. Luzzi, J. E. Fischer, D. A. Walters, M. J. Casavant, J. Schmidt, R. E. Smalley, Appl. Phys. Lett. **77** (2000) 663
[49] M. Knupfer, T. Pichler, M. S. Golden, J. Fink, A. Rinzler, R. E. Smalley, Carbon **37** (1999) 733
[50] M. Knupfer, Surface Science Reports **42** (2001) 1
[51] S. Valencia, H. Ch. Mertins, D. Abramsohn, A. Gaupp, W. Gudat, P. M. Oppeneer, Physica B. Condensed matter, Physica B **345** (2004) 189
[52] Y. Maniya, R. Fujiwara, H. Kari, H. Tou, E. Nishibori, M. Takata, M. Sakata, A. Fujiwara, X. Zhao, S. Iijima, Y. Ando: Phys. Rev. B **64** (2001) 073105
[53] S. J. Roosendaal, B. van Asselen, J. W. Elsenaar, A. M. Vredenberg, F. H. P. M. Habraken, Surf. Sci. **442** (1999) 329